A Self-evolution Hybrid Robot for Dental Implant Surgery

Yuan Feng[1], Min Chen[1], BaoXin Tao[2], ShiGang Wang[1], JinQiu Mo[1],
YiQun Wu[2], and QingHua Liang[1(✉)]

[1] School of Mechanical Engineering, Shanghai Jiao Tong University,
Dongchuan Road 800, Minhang District, Shanghai 200240, China
qhliang@sjtu.edu.cn

[2] Department of Second Dental Center, Shanghai Ninth People's Hospital,
College of Stomatology, School of Medicine, National Clinical Research Center
for Oral Disease, Shanghai Key Laboratory of Stomatology and Shanghai Research
Institute of Stomatology, Shanghai Jiao Tong University, 639, Zhizaoju Road,
Shanghai 200011, China

Abstract. Dental implant surgery is an effective method for remediating the loss of teeth. A novel custom-built hybrid robot, combining the advantages of serial manipulator and parallel manipulator, was proposed for assisting the dental implant surgery. The hybrid robot is comprised of 3 DOF translation joints, 2 DOF revolute joints and a Stewart manipulator. The translation joints are used for initial position adjustment, making the Stewart manipulator near the target position. The revolute joints are used for assisting the Stewart manipulator in initial orientation adjustment. The procedure of robot-assisted dental implant surgery is designed and described. Considering the limited workspace of Stewart manipulator, we set minimizing the joint displacement of the Stewart manipulator as the optimization objective to find an optimal joint configuration during initial orientation adjustment. In order to find the optimal joint configuration quickly, neural network is used to map the relationship between the target orientation and the optimal joint configuration. In addition, a self-evolution strategy is proposed for optimizing the learning model continuously. And the effectiveness of the strategy is validated in the phantom experiment.

Keywords: Robot-assisted dental implant surgery · Hybrid robot · Neural network · Self-evolution strategy

1 Introduction

Dental implant surgery has been recognized as a standard of care for remediating the loss of teeth [1]. The operation process involves in drilling a cavity and

---

placing an implant in the jawbone. The pose accuracy of drilling the cavity could influence the implant placement, which will increase the success rate of operation [2]. However, due to the possibility of human error, it is difficult to drill a cavity accurately.

Dental implant robot system was developed to satisfy the requirement of high precision for operation. Sun et al. [3] proposed an image-guided robot system for dental implant. The system comprises of a Coordinate Measurement Machine and a commercial 6 DOF serial robot Mitsubishi. A two-step registration is proposed to transform the planned implant insertion into robot target pose, guiding the robot perform the operation accurately. Cao. [4] used surgical navigation system for guiding an UR robot for zygomatic implant placement. With the help of surgical navigation system, the movement of patient can be tracked constantly, and the robot can adjust the target pose in real time. Phantom experiments were performed and it shows that compared with manual operation, robot can improve the pose accuracy of the cavity. J Li [5] design a compact serial robot based on tendon-sheath transmission, by which the actuators could be placed away from the manipulator. The robot adopted teleoperation technology, which allows the surgeon control the robot by a haptic device. Although the robot could relief burdens of surgeon, the accuracy of the cavity can only be guaranteed through the experience of doctors. Yomi [6] developed by Neocis company, is the first commercially available robot system for dental implant. It is a 6 DOF serial cooperative robot. After registration, the Surgeon can drag the robot to the target pose according to the visual guidance. Once the robot in the right orientation and position, it can guide the surgeon complete the drilling operation.

However, the structure of the above robots is all serial manipulator. Although the manipulator possesses large workspace, it has low stiffness, which may lead large deviation from the planned trajectory in the case of high feed force. Compared to serial manipulator, parallel robot has high stiffness and precision. While its workspace is limited, sometimes operation may not be completed.

In this study, we combine the advantages of parallel robot and serial robot, designing a novel hybrid robot system. The hybrid robot is composed of parallel manipulator and serial manipulator. The parallel manipulator is responsible for drilling the cavity due to its high stiffness. The serial manipulator is responsible for enlarging the workspace of parallel manipulator, assisting it in adjusting the pose of drill bit. In addition, we propose a self-evolution strategy to coordinate the motion relationship between serial and parallel manipulator.

2   Structure Design of the Robot

2.1   Structure Scheme

The structure scheme of the hybrid robot is shown in Fig. 1. The parallel manipulator is a 6 DOF Stewart platform, which could adjust the position and orientation of the end-effector. The serial manipulator is composed of three translation joints for assisting the Stewart manipulator in position adjustment, two revolute joints for assisting the Stewart manipulator in orientation adjustment.
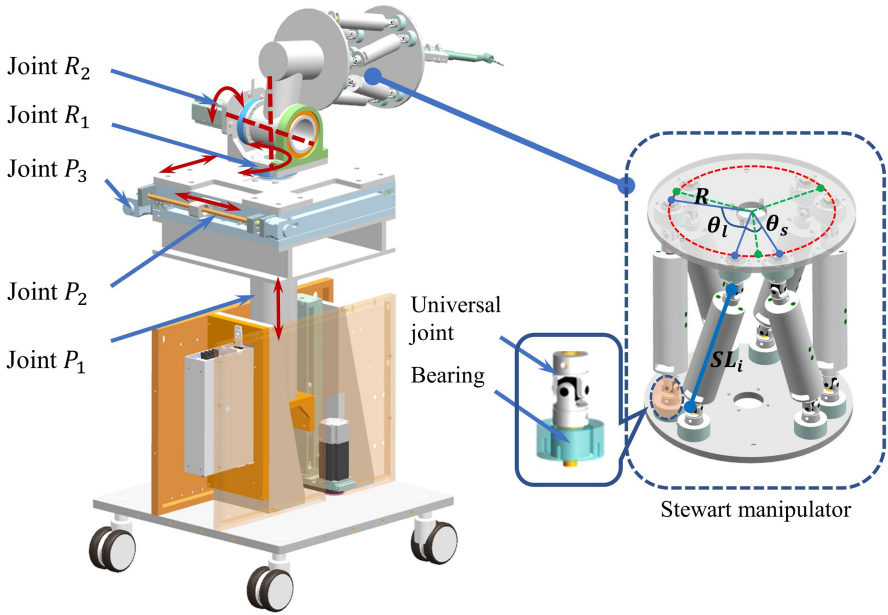
Fig. 1. Structure of the hybrid robot.

The three translation joints are actuated by three screw modules. The axes of the three translation joints are perpendicular to each other and decoupled, which could simplify the control. The first joint P_1 provides linear motion perpendicular to the ground. The motion range of P_1 joint is 0 to 200 mm, which determines overall height of the robot from 1220–1420 mm. Joint P_2 and joint P_3 provide planner motion, and the motion range of them is $-100 - 100$ mm, which is satisfied with the requirement of position workspace. The two rotation joints adopted gear drive, and the motion range of them is $-10° - 10°$. Joint R_1 is also used to switch between the initial state and the working state of the robot.

The Stewart manipulator is comprised of a moving platform, a fixed platform, and six prismatic joint. The base and the moving platform are connected by the prismatic joint by two equivalent sphere(S) joints. It is noticed that the equivalent sphere joint is composed of a universal joint and two angular contact bearings, increasing the loading capability, as Fig. 1 shows. The radius R of moving platform and fixed platform is the same, both of which is 190 mm. The equivalent sphere(S) joints are evenly distributed. The angle θ_s is 30° and θ_l is 90°. The motion of the moving platform is generated by the six prismatic joints, which could be denoted by SL_i (i = 1, 2, ..., 6). The motion range of the prismatic joint is 199.85–238.85 mm, and the initial position is 219.35 mm.
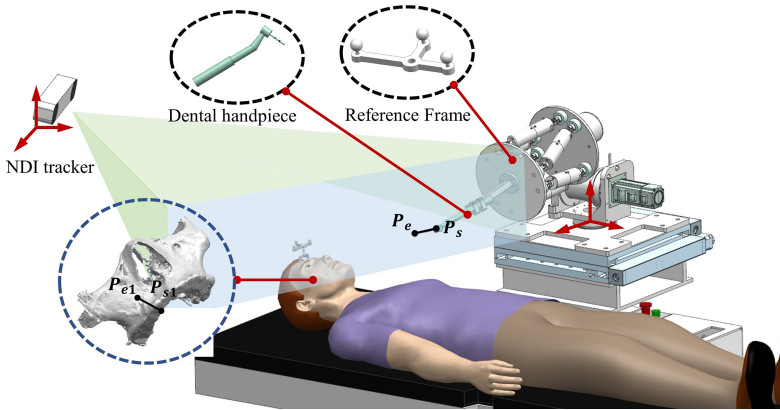
2.2   Working Principle

Fig. 2. The working diagram of the robot.

The working principle is illustrated in Fig. 2. The hybrid robot is under the guidance of surgical navigation system. Robot and patient are attached to the passive optical frame. Through the optical tracking device (NDI, Northern Digital Inc.), the pose of robot and patient could be detected real time. Before robot operation, the planned drilling trajectory and the drill bit are transformed to robot base coordinate and denoted by two vectors $\boldsymbol{P_{s1}P_{e1}}$, $\boldsymbol{P_sP_e}$ respectively. $\boldsymbol{P_e}$ represents the tip of drill bit and $\boldsymbol{P_s}$ represents a point in the axis of drill bit. The length of $\boldsymbol{P_sP_e}$ is equal to the length of drill bit.

The robot operation has three steps:

(1) Initial orientation adjustment. The hybrid robot adjusts the orientation of drill bit $\boldsymbol{P_sP_e}$ parallel with the planned trajectory $\boldsymbol{P_{s1}P_{e1}}$
(2) Initial position adjustment. In order to ensure the safety motion of robot from the outside of oral cavity to the planned trajectory, physical human-robot interaction (PHRI) is applied. the surgeon drags the handpiece through PHRI to make the position of drill bit $\boldsymbol{P_s}$ near the start position $\boldsymbol{P_{s1}}$
(3) Stewart manipulator precise adjustment and cavity preparation. The parallel manipulator adjusts the drill bit to the start point, and performs the cavity preparation after surgeon confirm.

3   Self-evolution Strategy for Orientation Adjustment

3.1   Analysis of Orientation Adjustment

During initial orientation adjustment, two revolute joints and Stewart manipulator are involved. The orientation of drill bit with respect to base coordinates could be determined by Eq. 1:

$$X_{dv} = f(\theta_1, \theta_2) F(x, y, z, \alpha, \beta, \gamma) * P_s P_e \tag{1}$$

According to Eq. 1, given a target vector X_{dv}, the computation of variable $X = (\theta_1, \theta_2, x, y, z, \alpha, \beta, \gamma)$ belongs to solving the underdetermined equations, which means there are infinite solutions. As Fig. 3 shows, different joint configurations correspond to the same orientation of the drill bit.

Considering the limited joint range of Stewart manipulator, if the joints approach the limit position after orientation adjustment, the Stewart manipulator may not complete the surgical operation. Therefore, among the infinite solutions, it is essential to find the proper solution that minimum the joint displacement. The problem may be solved by optimal algorithm, which could be presented as Eq. 2:

$$\begin{aligned} \min \| F_I(x, y, z, u, v, w) - SP_{\text{init}} \| \\ \text{s.t. } X_{dv} = F_I(\theta_1, \theta_2, x, y, z, \alpha, \beta, \gamma) * P_s P_e \\ \theta_{\min} \le \theta \le \theta_{\max} \\ SL_{\min} \le SL_i \le SL_{\max} \end{aligned} \tag{2}$$
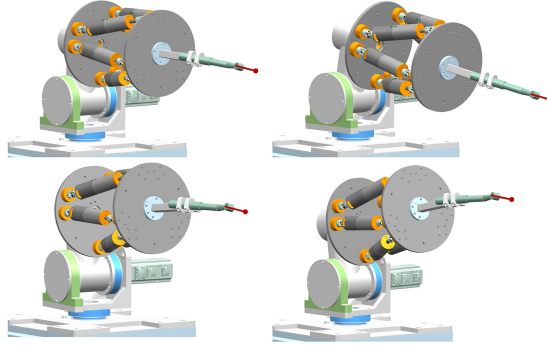

Fig. 3. Multiple solution for the same orientation.

After given the aim orientation, the optimal algorithm, for example genetic algorithm, could search in the joint space to find an optimal solution, minimizing the joint displacement. However, those algorithms are easily trapped in local minimum. In addition, the initial random solutions are often difficult to meet the constraints, which increase the exploration time.

Actually, from the Eq. 1, it could be found that once the variables (θ_1, θ_2) are determined, the pose of the Stewart manipulator is unique. Besides, if the distance between $\theta_i = (\theta_{1i}, \theta_{2i})$ and $\theta_{i+1} = (\theta_{1i+1}, \theta_{2i+1})$ is close, the corresponding joint displacement of Stewart manipulator is similar. Therefore, the revolute joint variables θ_i could be discretized and the global optimal solution could be derived by grid search in the variables space. However, grid search method often takes a lot of time, which is not suitable for robot control during surgery operation. An efficient solution is establishing a mapping function from the aim orientation to the global optimal joints space.

Neural networks were capable of learning complex functions, which led to their use in applications including pattern recognition, function approximation, data fitting, and control of dynamic systems [7]. The multilayer perception neural network includes input layer, hidden layers, and output layer. In this study, the input is the desire orientation of drill bit $\boldsymbol{X}_{dv}$ The output is the corresponding global optimal joint variable $\boldsymbol{\theta}_{op}$. For feed forward, the output of the neurons are given by Eq. 3. According to the existing input and output data, it could learn the mapping function by updating the weights w_{ij} through backpropagation algorithm, as Eq. 4 shows.

$$\boldsymbol{\theta}_{\text{out}} = \varphi \left(\sum_j \boldsymbol{W_j} \varphi \left(\sum_k \boldsymbol{W_k} \varphi \right) \cdots \varphi \left(\sum_i \boldsymbol{W_i} \boldsymbol{X}_{dv} \right) \right) \qquad (3)$$

$$w_{ij} = w_{ij} + \frac{\partial \Delta \boldsymbol{E}}{w_{ij}} \qquad (4)$$

where $\phi(\cdot)$ is the activation function, $\Delta \boldsymbol{E}$ is the RMSE, which could be represented by:

$$\Delta \boldsymbol{E} = \frac{1}{2} \left(\boldsymbol{\theta}_{\text{out}} - \boldsymbol{\theta}_{\text{op}} \right)^2 \qquad (5)$$

After the neural network has been trained, it could be used for giving an approximate value for a new sample. However, the architecture of neural network is hard to design, requiring a lot of expert knowledge and taking ample time [8].

Haifengjin [9] had proposed an efficient neural architecture search method auto-keras, which is based on network morphism guided by Bayesian optimization. The method turns out to be better than other automated machine learning methods for regression [10]. There are five steps for searching the optimal model:

(1) Initial the neural network according to the type of input data and output data.
(2) Train the generated neural network on GPU and evaluate the performance on the dataset.
(3) According to the trained model and its performance, update the surrogate model.
(4) The updated surrogate model generates new neural network by optimizing the acquisition function.
(5) The program returns to the second steps to train the new neural network and start the loop, until the stop criterion met.

In this study, we applied the method in our robot system as a self-evolution strategy for orientation adjustment. The algorithm flow is shown in Fig. 4.

Firstly, on the premise that the robot base coordinate system coincides with the human body coordinate system, we simulate the orientation of the drill bit in the robot base coordinate system. And then the corresponding optimal joint configuration is computed by grid search. Those values are added to the dataset and used for searching the first-generation neural network. Secondly,
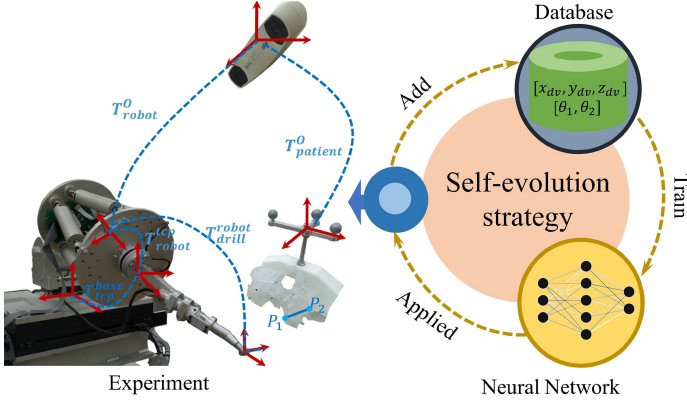
Fig. 4. Self-evolution strategy for orientation adjustment

we set up the phantom experiment as Fig. 4 shows. The robot is guided under the navigation system [11]. The orientation of the drill bit in the robot base coordinate could be derived by Eq. 6 and Eq. 7.

$$X_{dv}^{\text{robot}} = \left(T_{\text{robot}}^{0}\right)^{-1} T_{\text{patient}}^{o} P_1 P_2 \tag{6}$$

$$X_{dv}^{\text{base}} = T_{\text{tcp}}^{\text{base}} T_{\text{robot}}^{\text{tcp}} X_{dv}^{\text{robot}} \tag{7}$$

where $P_1 P_2$ represents the planned trajectory in the patient coordinate.

The trained neural network is applied in orientation adjustment during experiment. The robot system will record the experiment process. Finally, according to the recorded orientation of the drill bit, the global optimal joint configurations are computed. And the new values are added to the dataset, which are used for finding a better neural network model. Compared with traditional machine learning applied in robot kinematic [12–14], the self-evolution strategy could constantly explore more optimized learning model with the increase of data.

3.2   Experiment and Result

The orientation of the drill bit could be determined by the angle θ_s within $\pm 10°$ between the drill bit and the sagittal plane, θ_p within $70°\sim 90°$ between the drill bit and the jaw plane. Therefore, we could simulate the target orientation by selecting reasonable angle pairs (θ_s, θ_p) randomly and transforming the angle pairs to coordinate vectors according to geometry relationship. After getting the target orientation, the corresponding optimal joint configuration are found by grid search. In this study, 1910 target orientations are simulated, and the variables (θ_1, θ_2) are dispersed to a grid with $0.1°$ step size for grid search. The simulated dataset is divided into two subsets $(subd_1, subd_2)$ with the ratio 5:4. $subd_1$ is used for searching the first-generation neural network model. $subd_2$ are used for updating the trained neural network model to indicate the necessary of

self-evolution. For each subset, the ratio of training dataset to testing dataset is 4:1. Besides, we performed phantom experiments, and drilled 24 cavities to test the effectiveness of the self-evolution model.

During the training process, the input and output of the neural network are target orientation and optimal joint configuration respectively. The Relu activation function was used in the hidden layers. And the loss function is RMSE (root mean square error), as Eq. 5 shows. The exploration parameters are shown in Table 1.

Table 1. Exploration parameters

Parameter	Value
Number of layers	1, 2, 3, 4, 5
Number of neurons	16, 32, 64, 128, 256, 512, 1024
Dropout	0, 0.25, 0.5
Optimizer	Adam, SGD, Adam with weight decay
Learning rate	0.1, 0.01, 0.001, 0.0001

The first-generation neural network is shown in Fig. 5(a). The number of hidden layers is four layers. The number of neurons in the hidden layer is 64, 64, 256, 1024 respectively. The network weight is updated by Adam (adaptive moment estimation) optimization algorithm, and learning rate is set 0.001. Figure 5(b) shows the last-generation neural network. The number of hidden layers is four layers and the number of neurons in each layer is 64,64,64,64,128. During training, Adam is also used for updating the weight, and the learning rate is set 0.001. Figure 5(c)–(d) show the comparison of the error distribution between the first-generation neural network and the last-generation neural network. For the first joint variable, the most of the errors are concentrated around 0.192 for the first-generation neural network and 0.086 for the last-generation neural network. For the second joint variable, the most of the errors are concentrated around 0.713 for the first-generation neural network and 0.07 for the last-generation neural network. The result indicates that the last-generation after self-evolution has a better performance on predicting the joint configuration. Figure 5(e)–(f) shows the performance of the two neural network model in the phantom experiment. The error of the last-generation neural network is smaller than that of the first-generation neural network. The average error of the θ_1 is 0.42 for the first-generation model and 0.16 for the last-generation model. The average error of the θ_2 is 1.07 for the first-generation model and 0.38 for the last-generation model. The experiment shows that if the structure of the neural network isn't changed with the increase of the amount of data, the performance of the neural network on the new data is likely to be worse. It validates the effectiveness of self-evolution strategy.
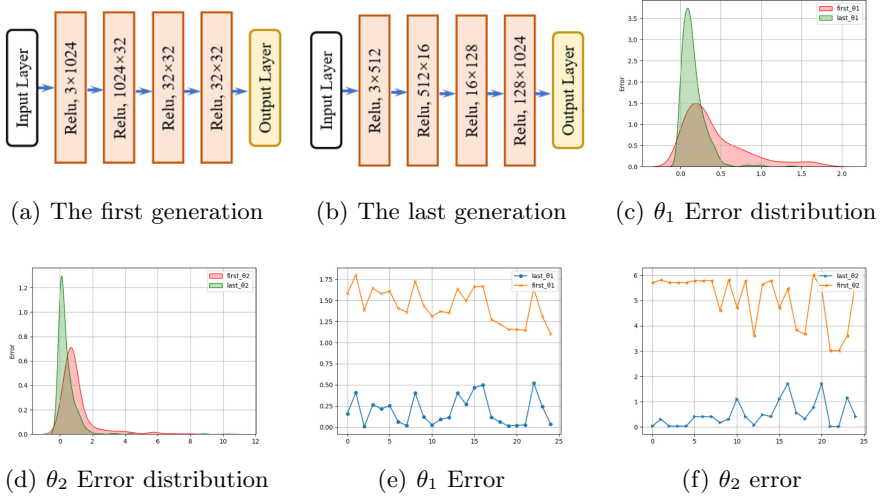
(a) The first generation   (b) The last generation   (c) θ_1 Error distribution

(d) θ_2 Error distribution   (e) θ_1 Error   (f) θ_2 error

Fig. 5. Experiment result

4   Conclusion

In this study, we developed a novel hybrid robot dedicated to dental implant. The hybrid robot consists of three translation joints, two revolute joints and a Stewart parallel manipulator. The Stewart manipulator is used for surgical operation considering the stiffness requirement of the robot. The three translation joints and two revolute joints are used to enlarge the workspace of Stewart manipulator. The corresponding operation flow for robot-assisted dental implant surgery is designed and could be divided into three steps: initial orientation adjustment, initial position adjustment and Stewart manipulator to complete surgical operation. During initial orientation adjustment, a neural network is used for finding the optimal joint configuration rapidly after given the target orientation. Besides, the neural network is updated by self-evolution strategy, which could learn the mapping relationship between the target orientation and the optimal joint configuration better and better. We manufactured the robot prototype, and integrated the robot system with the surgical navigation system to perform the phantom experiment. The phantom experiment validated the correctness of the robot kinematic model and the effectiveness of the self-evolution strategy.

References

1. Sun, X., Yoon, Y., Li, J., McKenzie, F.D.: Automated image-guided surgery for common and complex dental implants. J. Med. Eng. Technol. **38**(5), 251–259 (2014)
2. Wu, Y., Wang, F., Fan, S., Chow, K.F.: Robotics in dental implantology. Oral Maxillofacial Surg. Clin. North America **31**(3), 513–518 (2019)

3. Sun, X., Mckenzie, F.D., Bawab, S., Li, J., Yoon, Y., Huang, J.K.: Automated dental implantation using image-guided robotics: registration results. Int. J. Comput. Assist. Radiol. Surg. **6**(5), 627–634 (2011). https://doi.org/10.1007/s11548-010-0543-3

4. Cao, Z., et al.: Pilot study of a surgical robot system for zygomatic implant placement. Med. Eng. Phys. **75**, 72–78 (2020)

5. Li, J., et al.: A compact dental robotic system using soft bracing technique. IEEE Robot. Autom. Lett. **4**(2), 1271–1278 (2019)

6. Bolding, S.L., Reebye, U.N.: Accuracy of haptic robotic guidance of dental implant surgery for completely edentulous arches. J. Prosthet. Dent. (2021)

7. Köker, R., Öz, C., Çakar, T., Ekiz, H.: A study of neural network based inverse kinematics solution for a three-joint robot. Robot. Auton. Syst. **49**(3), 227–234 (2004). Patterns and Autonomous Control

8. Leiva-Aravena, E., Leiva, E., Zamorano, V., Rojas, C., Regan, J.M.: Neural architecture search with reinforcement learning. Science of the Total Environment (2019)

9. Jin, H., Song, Q., Hu, X.: Auto-Keras: an efficient neural architecture search system. In: Proceedings of the 25th ACM SIGKDD International Conference on Knowledge Discovery & Data Mining, pp. 1946–1956 (2019)

10. Truong, A., Walters, A., Goodsitt, J., Hines, K., Bruss, C.B., Farivar, R.: Towards automated machine learning: Evaluation and comparison of AutoML approaches and tools. In: 2019 IEEE 31st International Conference on Tools with Artificial Intelligence (ICTAI), pp. 1471–1479 (2019)

11. Chen, X., Ye, M., Lin, Y., Wu, Y., Wang, C.: Image guided oral implantology and its application in the placement of zygoma implants. Comput. Methods Programs Biomed. **93**(2), 162–173 (2009)

12. Limtrakul, S., Arnonkijpanich, B.: Supervised learning based on the self-organizing maps for forward kinematic modeling of Stewart platform. Neural Comput. Appl. **31**(2), 619–635 (2019). https://doi.org/10.1007/s00521-017-3095-4

13. Gao, R.: Inverse kinematics solution of robotics based on neural network algorithms. J. Ambient. Intell. Humaniz. Comput. **11**(12), 6199–6209 (2020). https://doi.org/10.1007/s12652-020-01815-4

14. Jiménez-López, E., de la Mora-Pulido, D.S., Reyes-Ávila, L.A., de la Mora-Pulido, R.S., Melendez-Campos, J., López-Martínez, A.A.: Modeling of inverse kinematic of 3-DOF robot, using unit quaternions and artificial neural network. Robotica **39**, 1230–1250 (2021)